

Influence of laser-induced for modification of polyacrylonitrile membranes by grafting of 2-hydroxyethyl methacrylate in the presence of visible light photoinitiator

Zeinab Khani-Arani, Ahmad Akbari*

Institute of Nanoscience and Nanotechnology, University of Kashan, Kashan, Iran, Tel. +98 31 55913154; emails: akbari@kashanu.ac.ir (A. Akbari), z.khani3045@gmail.com (Z. Khani-Arani)

Received 1 February 2022; Accepted 14 July 2022

ABSTRACT

In this article, a simple and cost-effective way introduce to modify polyacrylonitrile membranes and increase their efficiency. In the new method, the laser beam effect is used to graft 2-hydroxyethyl methacrylate monomer to prepare nanofiltration membranes. Azo dye is used as a visible light photoinitiator to absorb the radiation and create free radicals during the membrane modification. The laser-modified membrane analysis is performed by infrared spectroscopy, atomic force microscopy, scanning electron microscopy, contact angle, and zeta potential analysis. A significant decrease in the membrane charge from 1.17 to -6.91 mV indicates the proper performance of this method. Improvement surface hydrophobicity could be detected by contact angle measurement. The separation performances of salts proved that membranes are associated with charged nanofiltration separation behavior. The modified membrane has reached a suitable value in salts separation performance (83% Na_2SO_4 , 71% MgSO_4 , 36% NaCl, and 31% CaCl₂) and organic compounds separations of 94.3% Acid Blue 92, 89.4% Acid Orange 7, 88.9% ibuprofen, and 82.1% cefixime. As far as has been investigated, this process has not been used for the preparation of nanofiltration-based membranes up to now. It may open up new opportunities to introduce a different class of membrane materials.

Keywords: Polyacrylonitrile membranes; Nanofiltration; 2-hydroxyethyl methacrylate (HEMA); Laser; Graft polymerization; Visible light photoinitiator

1. Introduction

Among the conventional methods for wastewater treatment, separation processes using membrane technology as one of the most promising technologies have become very important in recent years and for reasons such as easy construction, ease of operation, and less energy consumption, widely used in the chemical industry, pharmaceutical companies, energy storage, energy conversion and also in environmental protection [1,2]. In general, polymeric membranes play a vital role in various areas from health care to water production, and considerable research has been done to understand their nature and improve their performance

[3]. Nanofiltration (NF) is a useful pressure-driven technique for molecular separation and its applications extended to different industrial fields such as food processes, petroleum, and pharmaceutical separations [4]. Most NF membranes are thin-film composite (TFC) membranes made of an active layer on top of porous support that determines the membrane separation function [5]. Numerous methods for membrane surface modification considered for the preparation of TFC NF membranes include interfacial polymerization [6], surface coating [7], layer-by-layer self-assembly [8], graft polymerization [9,10], etc. Membrane surface modification is a perfect advance to produce a membrane

* Corresponding author.

with better performance [11,12]. Surface modification by graft polymerization is a valuable process for the improvement of membrane surface properties by binding polymer chains onto a polymer membrane [13–15]. In graft polymerization, the monomer reacts with a membrane surface that is activated, thus improving the existing polymer membrane with new characteristics such as hydrophilicity, adhesion, anti-fouling, and conductivity [16]. The functional groups in the graft are introduced into the polymer substrate by irradiation and then establish a chain with the polymer through a chemical reaction or bonding of free radicals [17]. Therefore, the membrane surface can be modified arbitrarily through surface grafting modification with the desirable group. Various technologies are applied to surface modification of the membrane through the graft method, including plasma, electron beam-irradiated, and photopolymerization [18–21]. Excimer lasers with a wavelength of less than 400 nm have been worked so far [16,22–24]. At present, the use of LASER (light amplification by stimulated emission of radiation) with unique features, has penetrated almost all fields [25]. Its applications in medicine for the diagnosis and treatment of diseases [26], in communication and telecommunication devices [27], in cutting [28], carving [29], and in other parts of the industry, are unavoidable. By laser excitation, a molecule can absorb photons and excited state A^* is formed. In different ways, when $[A^*] > [A]$ stimulated emission occur [Eq. (1)] [30].



But so far radiation with a wavelength longer than 400 nm has not been practiced to improve the membrane surface and grafting. For a high wavelength to be effective in membrane surface modification, it seems necessary to use a visible light photoinitiator. Generally, a photoinitiator (PI) is a compound that can absorb ultraviolet (UV) or visible light and convert light energy into chemical energy to start a photopolymerization reaction in the form of initiator species such as free radicals [31]. Visible light PIs are strong dye compounds that can act as a photosensitizer. Recently, these structures with appropriate features such as safety and controllability, considered and can be an alternative to ultraviolet light PIs [32,33]. Azo dyes are one of the most important classes of synthesized organic dyes that include versatile applications [34]. These compounds

contain a double bond $N=N$ and are able to absorb visible and near-infrared (NIR) light [35,36]. Acid Red 114 (AR114) is a sort of azo dye with the ability to receive radiation in the infrared field and besides having azo bonds can form radical species [37,38] to start the reaction and facilitates the polymerization process on the membrane surface through IR waves. In this work, AR114 was chosen as an initiator to modify the surface of polyacrylonitrile (PAN) membrane. PAN-based membranes have suitable properties such as hydrophilicity, solvent stability, availability, and low cost in the process and are widely used for various applications [39–42]. However, surface modification to improve performance is still a challenge. Among monomers, 2-hydroxyethyl methacrylate (HEMA) can use for this purpose because of its hydroxyethyl pendant group. Therefore, it improves hydrophilicity and fouling resistance in the membrane. HEMA is known as a hydrophilic, non-toxic, and biocompatibility monomer [43] that is polymerized using various methods such as free radical, anionic, and controlled/living polymerization [44,45]. In this method, for the first time, a high-wavelength physiolaser is employed for grafting HEMA on PAN membrane *via* using azo dye as a visible light photoinitiator and optimizing its performance. This method has the great advantage of achieving modification in one single step.

2. Experimental

2.1. Materials and apparatuses

All reactions were carried out under an inert atmosphere. All chemicals used were of reagent grade. The materials and equipment used are listed in Table 1. This research tried to use the least and most economical materials, so discarded wastes were used to prepare the base membrane.

The influence of concentrations of HEMA (1, 2, 3, and 4 wt.%), number of pulses (1, 2, 3, and 4), and AR114 concentrations (30, 50, 70, 100 ppm) were investigated and were denoted as $M_{i,j,k}$ where i,j,k are the corresponding HEMA concentration, number of pulse and dye concentration, respectively (presented in Table 2).

2.2. Fabrication of PAN membranes

First, the solution containing PAN fibers (18% (w/w)), PEG2000 (4%) as pore former, and dimethylformamide

Table 1
Materials and equipment used

Designation	Description	Source
PAN	Polyacrylonitrile	Fibers made from textile waste
PEG (400, 600, 1000, 1500, 2000, 3000)	Polyethylene glycol	Merck, Germany
DMF	Dimethylformamide	Chem Lab, Belgium
HEMA	2-hydroxyethyl methacrylate	Merck, Germany
AR114	Acid Red 114	Yazd Alvan, Iran
–	Physiolaser	Globus, Italy
Na_2SO_4 , $MgSO_4$, NaCl, $CaCl_2$	Sodium sulfate, magnesium sulfate, sodium chloride, calcium chloride	Merck, Germany

Table 2
Membranes with different polymerization conditions and compositions

Membrane	HEMA concentration (wt.%)	Number of pulse	AR114 concentration (ppm)
M _{0,0,0}	–	–	–
M _{1,2,2}	1	2	50
M _{2,2,2}	2	2	50
M _{3,2,2}	3	2	50
M _{4,2,2}	4	2	50
M _{2,1,2}	2	1	50
M _{2,3,2}	2	3	50
M _{2,4,2}	2	4	50
M _{2,2,1}	2	2	30
M _{2,2,3}	2	2	70
M _{2,2,4}	2	2	100

(DMF) as solvent was prepared under reflux conditions and mixed by a magnet with a rate of 250 rpm for 24 h at 75°C. Thereafter, the prepared polymer solution was subjected to ultrasonic waves for 15 min and then cast on flat glass plates with a thickness of 255 μm by an adjustable casting knife. As mentioned, to the effect of laser in the grafting process, it is necessary to use visible light photoinitiator in an aqueous solution (as a non-solvent). Therefore, the stretched polymer film is soaked in an aqueous solution containing 50 ppm of AR114 for 24 h to prepare it for grafting by monomer. Water flux and permeability factor for the unmodified membrane (M_{0,0,0}) were calculated higher than 555.55 L m⁻² h⁻¹ and 185 L m⁻² h⁻¹ bar⁻¹, respectively, and it showed a rejection of less than 5%.

2.3. Laser-induced graft polymerization

The laser applied in this study has the following characteristics:

Physiolaser 1000 (Globus) with the wavelength of 808 nm, power of 1,000 W, output energy equivalent to 12.8 J cm⁻², and the radiation duration of each pulse was 2.7 min. Since the laser radiation is spot-on, a scanner with a speed of 0.17 cm s⁻¹ is used to work on the membranes. The membrane was dried and put in the monomer reservoir. Then the raw membrane was irradiated by different pulses of the laser. Upon laser excitation, a graft reaction is performed between the membrane and the monomer. Afterward, the modified membranes were washed with water and kept wet at room temperature.

2.4. Membrane morphological investigation

The surface properties of membranes were determined using SEM (scanning electron microscope, MIRA3 TESCAN) images. AFM (atomic force microscopy, CP II/Veeco, USA) was also used to analyze the surface of modified membranes. The chemical structure of the PAN

membranes was analyzed by Fourier-transform infrared (FTIR, IBB Bomem MB-100, Canada) spectroscopy measurements.

2.5. Membrane surface hydrophilicity study

The contact angle of water is usually used as an indicator to express the hydrophilicity of the membrane surface [46]. In this work, the contact angle was measured by Camera Model CAG-20. The surface charge was calculated by zeta potential (ZP) measurements (BROOKHAVEN OMNI/nano-book).

2.6. Nanofiltration experiments

For the permeation experiments, a cross-flow filtration system was used to measure the performance of the membrane. The operation pressure (ΔP) was 3 bar and the surface area of the membrane (A) in the cell was about 22 cm². For measuring the water flux (F) and permeability factor (L_p) (according to Eqs. (2), (3) [47]), about 6 L of pure water was added to the tank and filtrated with the modified membrane. After about 20 min, when the amount of permeation flux was stable, water volume was measured for 5 min. For report rejection of membrane, solutions with a concentration of 80 ppm of drugs, 60 ppm of dyes, and 0.01 M of salts are added, in the same way. Then the rejection can be calculated as Eq. (4) [47].

$$F = \frac{V}{A \times t} \left(\frac{L}{m^2 \cdot h} \right) \quad (2)$$

$$L_p = \frac{F}{\Delta P} \left(\frac{L}{m^2 \cdot h \cdot bar} \right) \quad (3)$$

The feed solution was pumped at 25°C and the applied pressure of ΔP . V is the volume of flux collected over a period of time (t) from the membrane.

$$R_{\text{obs}} (\%) = \left(1 - \frac{C_p}{C_f} \right) \times 100\% \quad (4)$$

where C_p and C_f refer to the feed and the permeate solution concentration to achieve retention rate (R).

The membrane performance can be characterized by determining the molecular weight cut-off (MWCO). The MWCO corresponded to 90% removal for polyethylene glycol (PEG) solutes with different molecular weights [48]. It was analyzed by a UV-Visible spectrophotometer (GBC Scientific Equipment Ltd., – Cintra 101 – UV-Visible Spectrometer, Australia) at a wavelength of 535 nm according to the method of Sabde et al. [49].

3. Result and discussion

3.1. FTIR analysis

Fig. 1 shows the IR spectrum of the basic membrane and the irradiated membrane with 2 pulses of laser. The spectrum of the PAN membrane shows sharp peaks

at 2,243; 1,736 and 1,628 cm^{-1} , which are for the stretching vibrations of the $-\text{C}\equiv\text{N}$, $-\text{C}=\text{O}$, $-\text{C}=\text{N}$ bands. The adsorption peaks at 2,932 and 1,449 cm^{-1} are assigned to the stretching and bending vibration of the $-\text{CH}$ and the $-\text{CH}_2$ groups, respectively. The broad peak at 3,628 cm^{-1} is due to the stretching vibration of the OH group. The presence of peaks related to carboxyl and hydroxyl in the spectrum of the base membrane is due to the use of textile waste has a mixture of PAN and PA in this work. However, the peaks of these two functional groups can be clearly observed in the spectrum of the modified membrane (Fig. 1b), which has been grown due to their presence in the monomer (HEMA).

3.2. SEM images

Through laser irradiation of the membrane, the monomer is attached to the surface of the membrane. SEM micrographs of basic and modified membranes (Fig. 2) confirm the formation of a thin and dense polymer layer on the top of PAN. The prepared membranes observe a finger like cross-section. In addition, while displayed in Fig. 2b, the ablation of the surface by laser irradiation creates layer-by-layer structures that coat the surface of the membrane and narrow the membrane pores.

The active layer and cross-section morphology of the membranes are shown in Fig. 3. A smooth layer is formed by laying the membrane in the monomer solution and making polymerization on the surface. This layer covers some of the membrane pores and reduces the porosity of the membrane. With the formation of denser skin layers with increased thickness, the surface of the substrate membrane is arranged and evened.

3.3. AFM results

Membrane roughness was evaluated by surface topography with AFM analysis. Increasing the roughness leads to an increase in membrane fouling, possibly because it has higher chemical activity and reaction ability [50]. The results of AFM are presented in Fig. 4. The roughness parameters express that a smooth surface with fewer chances of fouling is achieved in presence of HEMA as compared to the unmodified membrane. Raw membrane roughness is 477.3 nm, while modified PAN shows a unique surface structure with 74.05 nm roughness. After polymerization onto the microporous support surface homogeneous and fine structures formed. The results from AFM parameters are consistent with the morphologies observed by SEM images.

3.4. Contact angles

Decreasing the contact angle is one of the most significant results of this research. Reducing the contact angle increases the hydrophilicity of the modified membrane surface. Since by laser treatment, monomer hydrophilic functional groups are attached to the membrane surface, the hydrophilicity of the membrane surface raises and, as shown in Fig. 5, the contact angle decreases from 66.7° to 54.0°.

3.5. Zeta potential

As negatively charged membranes lead to a higher rejection of anion and additionally to avoid membrane fouling, it is of major importance to create a negative

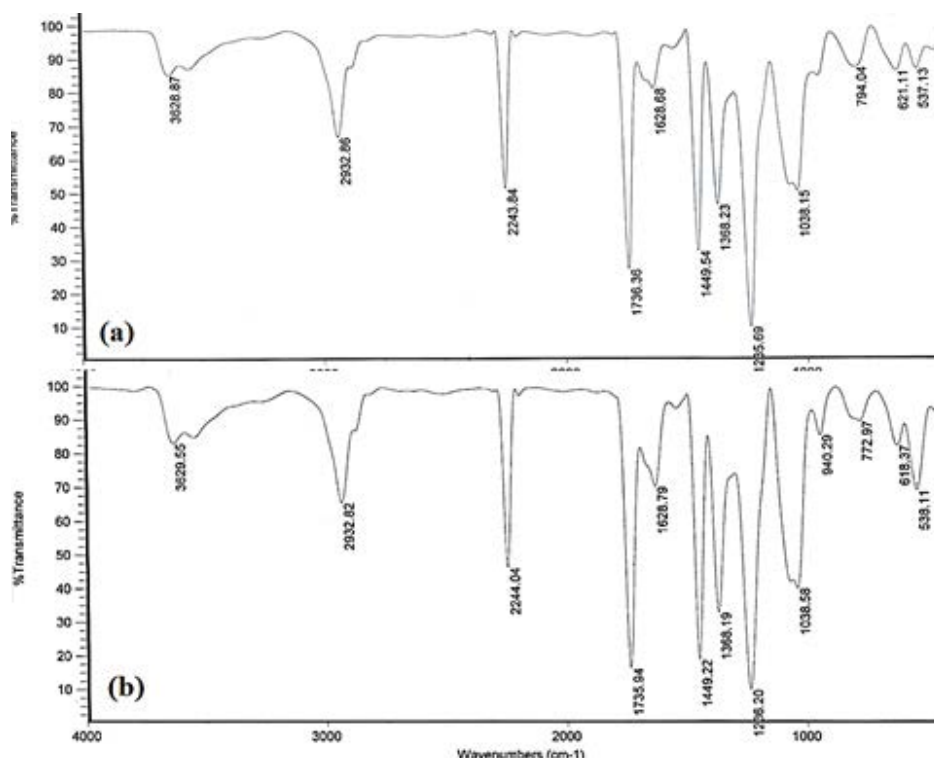


Fig. 1. FTIR spectra of (a) basic membrane and (b) modified membrane.

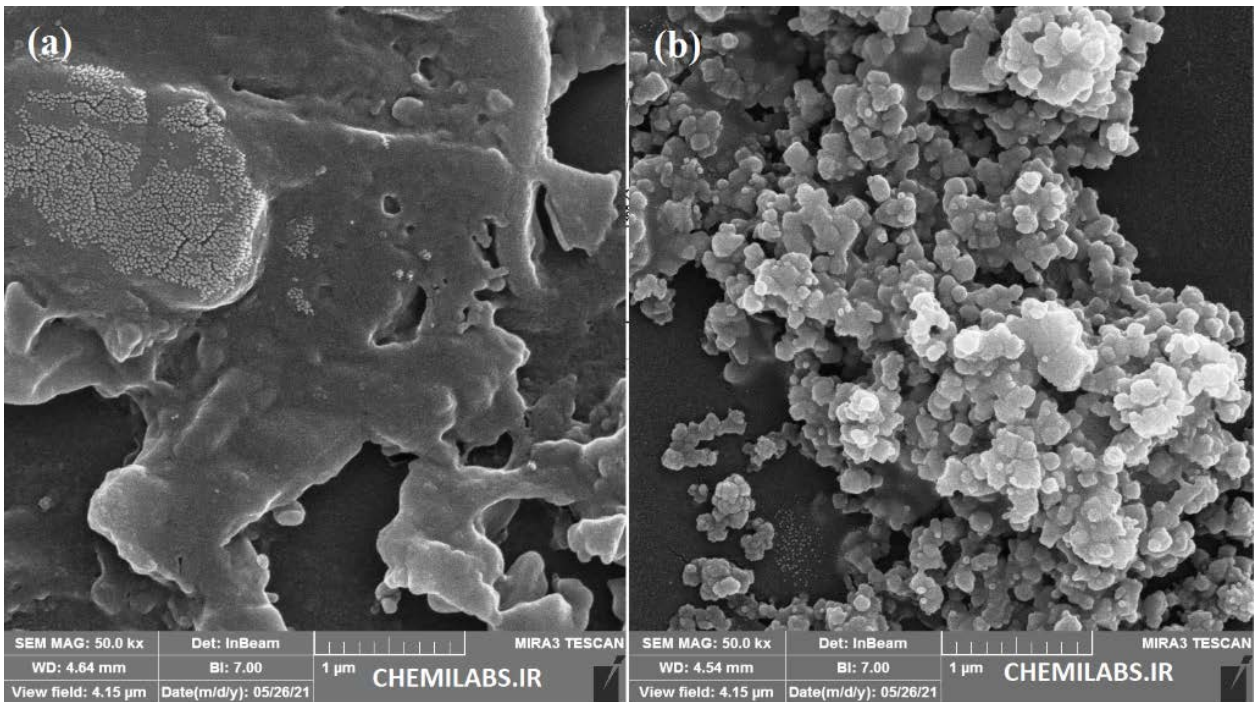


Fig. 2. SEM images of (a) basic membrane and (b) modified membrane.

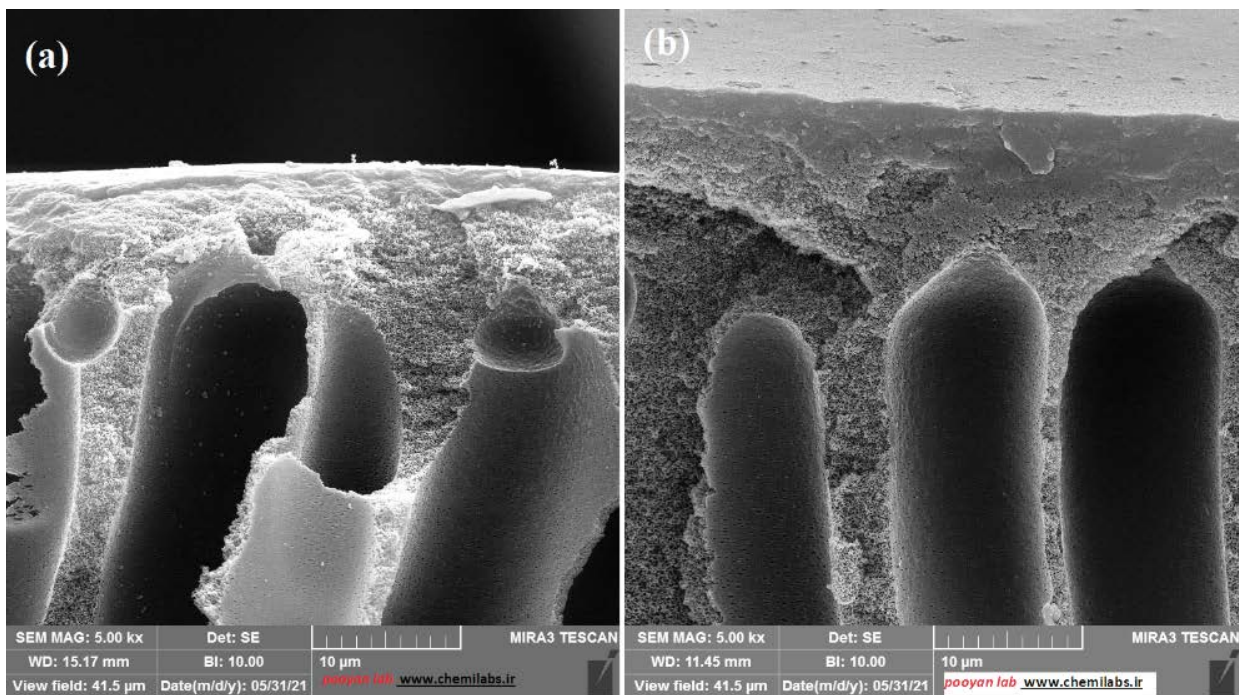


Fig. 3. Cross-section of morphology of (a) basic membrane and (b) modified membrane.

surface charge in the modified membranes with a reliable method. Zeta potential is capable of describing the surface charge of the membrane and as surface charge strongly influences the rejection of some compounds, the zeta potential is an essential tool for modified membrane characterization. Results from the measurement of

the zeta potential are presented in Table 3. The modified membrane showed a clear shift between positive and negative surface charges from about 1.17 mV to about -6.91 mV. The high density of negative charges on the surface of the polymer is due to the presence of anionic groups in the linked monomer.

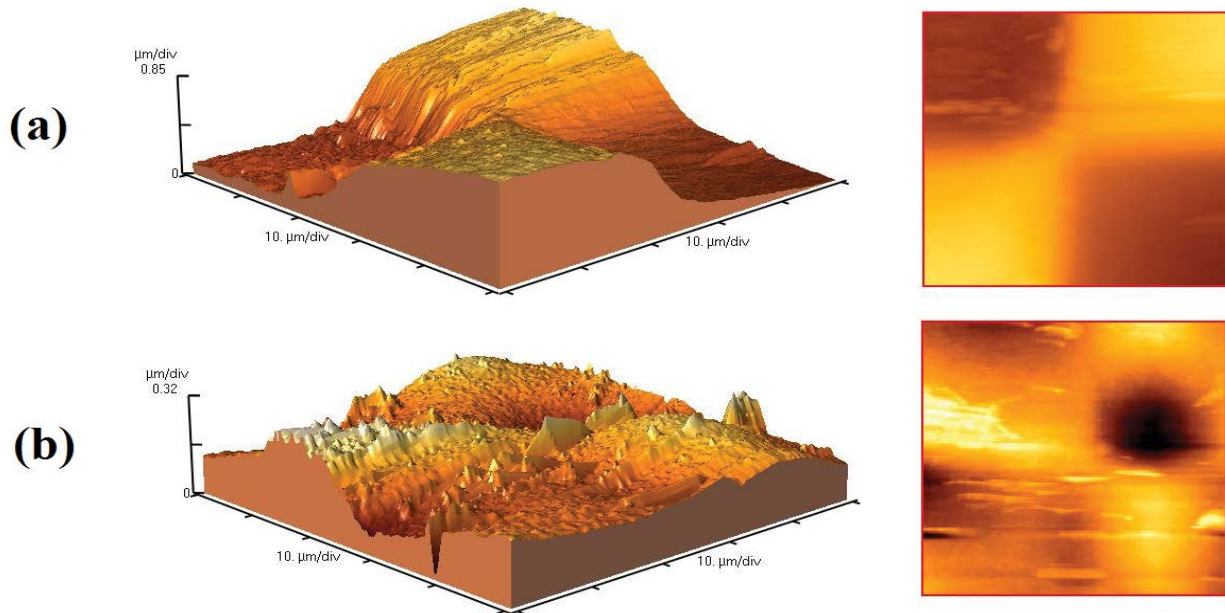


Fig. 4. AFM images of (a) basic membrane and (b) modified membrane.

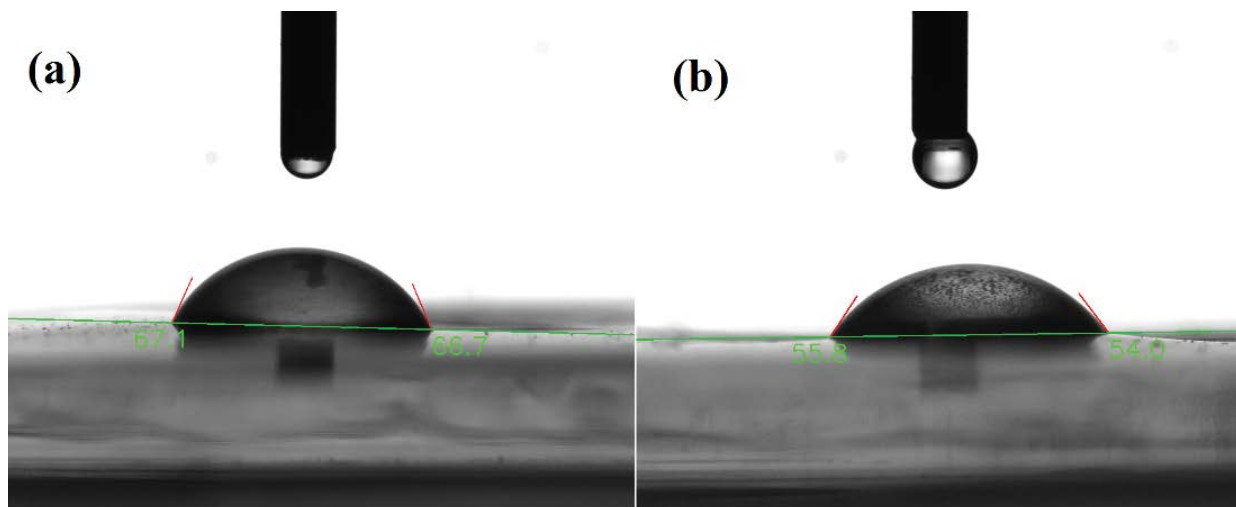


Fig. 5. Contact angle of water before and after laser treated on polyacrylonitrile membrane.

3.6. Provisional mechanism

In this research, since the laser wavelength utilized is in the infrared range and cannot perform monomer grafts on the membrane surface, Acid Red 114 (AR114) has been used as a photoinitiator to create active species. Fig. 6 displays the molecular structure of employed reactants during this method. Fig. 7 shows the possible radical structures created after laser light on the AR114, which as a photoinitiator, operates the reaction. Then, according to the proposed mechanism presented in Fig. 8, the polymerization process continues then the grafting on the membrane surface is favorably performed.

The outcomes revealed that the photoinitiator system including AR114, base membrane, and monomer has

satisfying efficiency for surface modification. So the use of AR114 with the mentioned capabilities is one of the possible solutions to produce active species in the reaction.

3.7. Separation performance of membranes

Reaction conditions for membrane synthesis were studied in various trends. Fig. 9 shows the permeability factor (L_p) of membranes prepared at different HEMA concentrations through 2 pulses of laser. With the increase of monomer concentration from 2 to 4 wt.%, the L_p continuously increased from 12.03 to 16.66 $L m^{-2} h^{-1} bar^{-1}$. The monomer solution absorbs more radiation at higher concentrations and limits its proper absorption by the

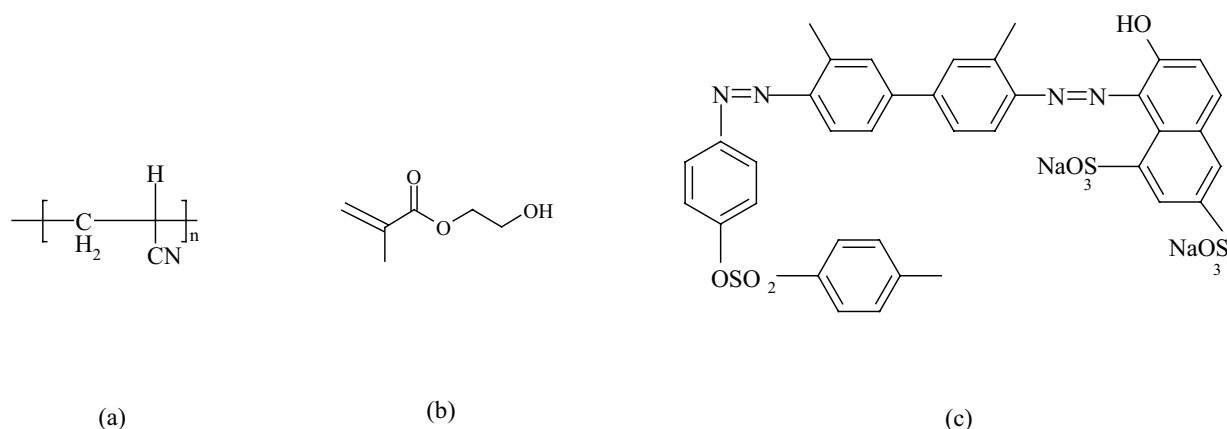


Fig. 6. Molecular structure of PAN (a), HEMA (b) and AR114 (c).

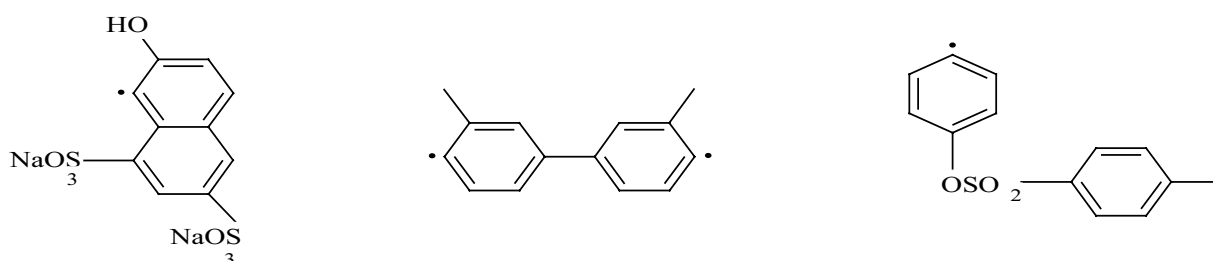


Fig. 7. Radical structures of the AR114 after laser irradiation.

membrane surface. A suitable amount of monomer is not available for the reaction at a concentration of 1 wt.%. So an increase in the coefficient is observed.

Laser exposure is a proper technique in the membrane grafting process. As disclosed in Fig. 10, the best membrane performance was observed for 2 pulses, at a constant concentration of HEMA. The reason for this probably is attributed to the degree of laser ablation. The long duration of the laser exposure will destroy the membrane surface and finally in an incomplete modification process.

Due to the presence of dye compounds in the membrane solution as visible light photoinitiators, the dye concentration is also studied and exhibits the best result at a concentration of 50 ppm (Fig. 11). Concentrations higher than 50 ppm of the dye applied in the monomer polymerization pathway and chain formation interfere.

Checking results show the modification process is altered the inner pore structure of the membrane which led to a decrease in the membrane porosity and a decline in permeability factor (L_p).

Salt rejection was examined to determine the performance of NF membranes. The separation performances of the membranes depend on pore size, surface roughness, hydrophilicity, and charge. The salt rejection behavior of the optimized membrane was measured for solutions of Na_2SO_4 , MgSO_4 , NaCl , and CaCl_2 as feed. NF membranes for bivalent ions with similar charges exhibit comparatively higher rejection than monovalent salts ($\text{SO}_4^{2-} > \text{Cl}^-$) and vs. do the opposite for dissimilar charges ($\text{Na}^+ > \text{Ca}^{2+} > \text{Mg}^{2+}$).

Table 3
Zeta potential measurement

Membrane	Zeta potential (mV)	pH
$M_{0,0,0}$	1.17	5.697
$M_{2,2,2}$	-6.91	5.815

The optimized membrane in Fig. 12, displayed the highest rejection of about 83% for Na_2SO_4 and the lowest rejection of 31% for CaCl_2 .

A comparison of the optimized membrane with other membranes by different concentrations and irradiation times shows that the optimized membrane records provided more salt rejection. This result revealed that the effect of laser improved the rejection of salts in the presence of 2 wt.% HEMA by 2 pulses.

3.8. Determination of the MWCO

For better comprehension of the effects of the modification on membrane properties, the rejection of different molecular weight substances was measured by the membrane filter. For this purpose, 1000 ppm solutions of PEG standards with different molecular weights were used to determine the MWCO. The MWCO of the surface-modified membrane by PEG rejection analysis was obtained at about 2300 Da (Fig. 13).

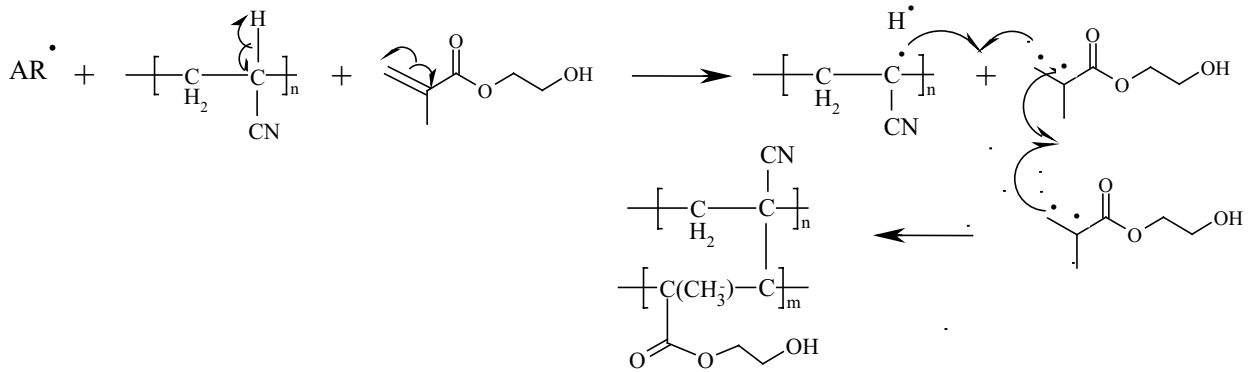
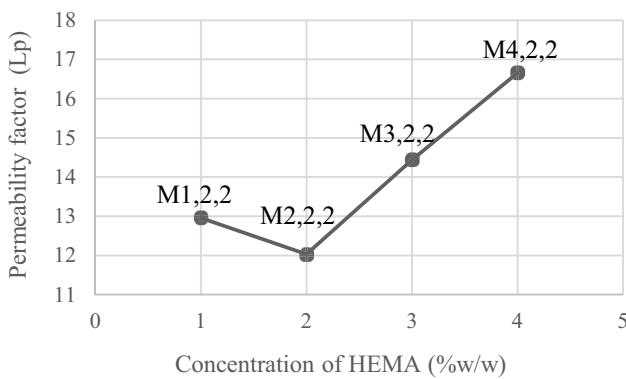
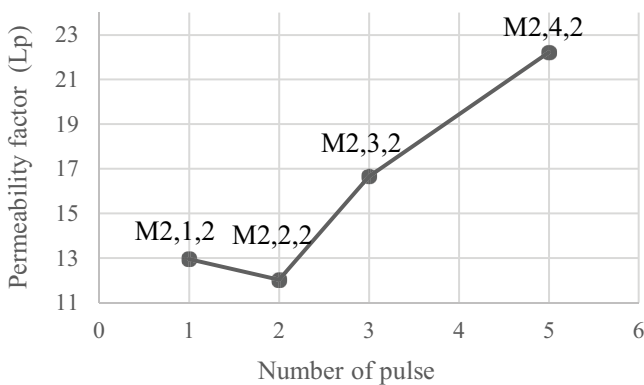


Fig. 8. Schematic of provisional grafting mechanism PAN membrane.

Fig. 9. Influence of monomer concentration on permeability factor (L_p) through 2 pulses of laser.Fig. 10. Effect of the number of pulses on permeability factor (L_p) at concentration of 2 wt.% HEMA.

3.9. Measurement of performance of modified membranes

Separation tests of several organic compounds are performed to evaluate the modified membrane performance. Their physicochemical properties and chemical structure are summarized in Table 4. As discussed, $M_{2,2,2}$ have higher performance. Hence, this modified membrane was intended for rejection testing.

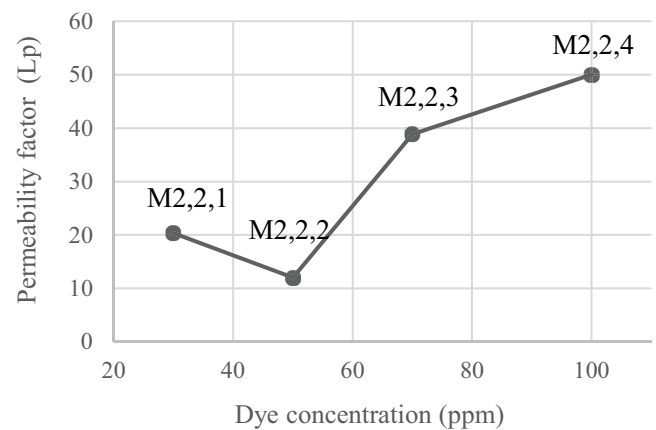
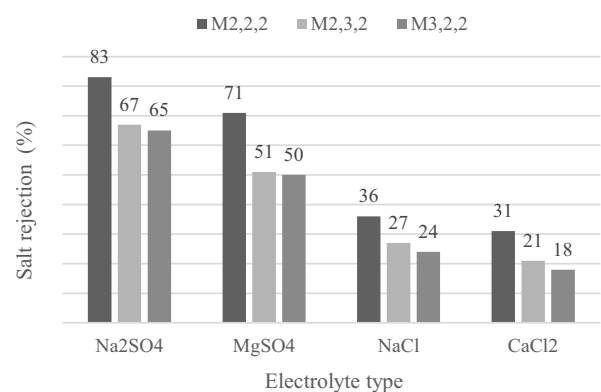


Fig. 11. Effects of the azo dye concentration (AR114) in membrane solution.

Fig. 12. Rejection of different membranes to different electrolytes (Na₂SO₄, MgSO₄, NaCl, and CaCl₂).

Chosen compounds with certain concentrations were employed as feed to evaluate the rejection of the membrane surface. Its surface absorption was observed before and after the filtration process through 3 bar pressure by UV-VIS absorption spectrophotometer.

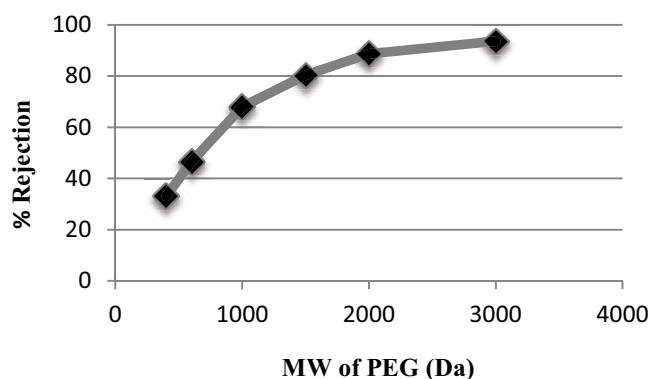


Fig. 13. MWCO of $M_{2,2,2}$ as optimal modified membrane.

Fig. 14 presents the rejection test of several pollutants on the surface of the membrane after grafting. The order in the rejection test is cefixime < ibuprofen ≤ Acid Orange 7 (AO7) < Acid Blue 92 (AB92). The above order indicates that AB92 is the most rejected from the membrane, while cefixime is the least likely. The highest percent removals observed of AB92, AO7, ibuprofen, and cefixime were 94.3, 89.4, 88.9, and 82.1, respectively. This result intimates that the charge and sieving effect govern the separation of the compounds. The rejection value during nanofiltration relies on two parameters of pore size and ion charge [51]. AB92 due to the strong anionic groups and high molecular weight (MW) showed the highest rejection compared to others. AO7 and ibuprofen show the same value despite the different MW. This effect may be relevant to the presence of an amine group in AO7 that creates some positive charge in the solution while ibuprofen has active negative groups. The amine groups in cefixime (cationic in aqueous solutions), cause that in this molecule, even with high MW, less rejection occurs. It is well established that anionic pollutants absorb to membrane surfaces.

The fouling propensity of the treated membranes shown in Fig. 15. One of the important problems in membranes is fouling. Fouling is begun with the absorption of foulants in the feed solution onto the membrane surface and the internal structure, resulting in pore blocking and cake layer formation [52–55]. The fouling experiments were operated continuously for 180 min at 3 bar pressure at room temperature. For this purpose, 50 ppm solution of AB92 was selected as foulant. Then physical cleaning was conducted with DI water flushing. The filtration measures were continued in the second and third cycles for alike another time by the previous method. It should be noted that due to a large amount of flux and the permeability coefficient in the raw membrane, measuring the fouling test for it seems useless (the permeability factor of $M_{0,0,0}$ for all reagents = above $185 \text{ L m}^{-2} \text{ h}^{-1} \text{ bar}^{-1}$).

For permeate factor, steep flux decline behavior was not observed for the treated membrane, indicating the lowest fouling propensity. As can be detected from the data in Fig. 15, after the first and second washes, only 3% and 6%, respectively, of the first time cycle, a decrease in permeability coefficient is perceived. Thus, properties changes of the membrane surface by laser grafting polymerization of HEMA resulted in less anionic fouling propensity.

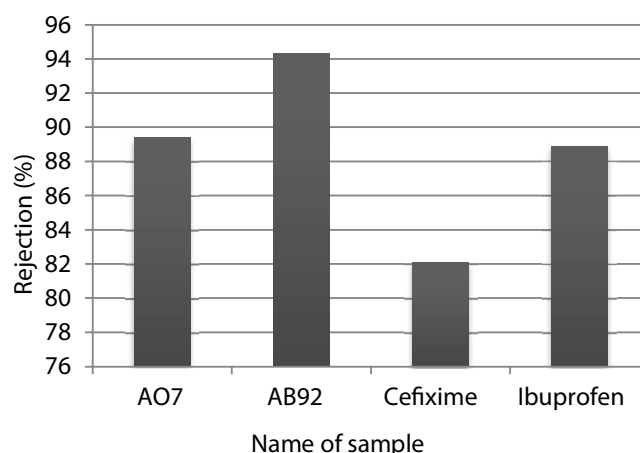


Fig. 14. Rejection of selected pollutants by modified membrane ($M_{2,2,2}$).

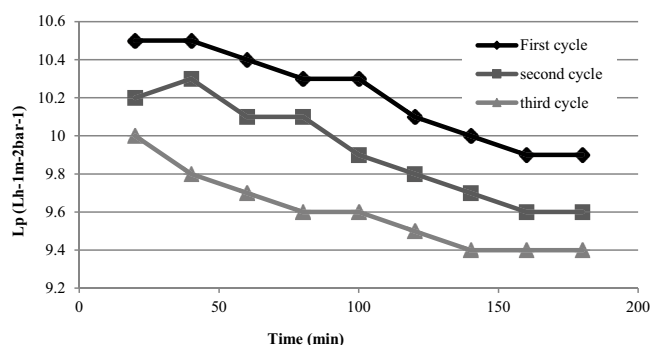
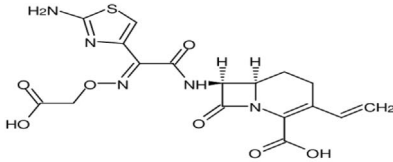
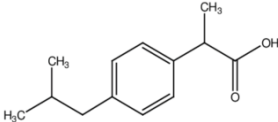
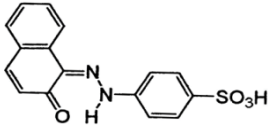
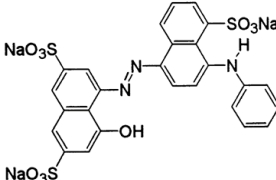


Fig. 15. Antifouling properties of $M_{2,2,2}$ compared to first and second washing and reuse.

4. Conclusion

In this study, for the first time, raw PAN membranes are modified by laser polymerization, which induced the addition of HEMA hydrophilic as a monomer on the membrane surface. For this purpose, Acid Red 114 is used as a visible light photoinitiator to start photopolymerization. Laser exposure pulse and monomer concentration after optimization were 2 pulses and 2 wt.%, respectively. Treated membranes showed significant performance improvement in reducing the membrane fouling phenomenon. The NF process resulted in the removal of 94.3% of AB92 and the removal of 88.9% of ibuprofen. TFC membrane prepared with PAN substrate shows 83% Na_2SO_4 rejection. Before and after treatment, SEM and AFM images of the membrane surface are provided as support information. The obtained images show the formation of a selectable and homogeneous thin layer, which reduces the roughness of the membrane surface. The reduction of the contact angle from 67.1° in the unmodified membrane to 52.5° in the modified PAN membrane indicates an increase in hydrophilicity after treatment. Measurement of zeta potential showed more negative surface charge (-6.91 mV) than the membrane before surface modification (1.17 mV). Due to the beneficial effect of this method on membrane

Table 4
Properties of the selected compound for measurement of rejection rate

Name of sample	Formula	Molecular structure	Molar mass (g mol ⁻¹)	concentration (ppm)
Cefixime	C ₁₆ H ₁₅ N ₅ O ₇ S ₂		453.440	60
Ibuprofen	C ₁₃ H ₁₈ O ₂		206.285	60
Acid Orange 7 (AO7)	C ₁₆ H ₁₁ N ₂ NaO ₄ S		350.32	50
Acid Blue 92 (AB92)	C ₂₆ H ₁₆ N ₃ Na ₃ O ₁₀ S ₃		695.58	50

properties and membrane performance, it is recommended that they be further studied.

Acknowledgment

The authors would like to especially thank the support of Khatam Al-Anbia Aran and Bidgol Physiotherapist Center with the management of Ibrahim Hasan Shiri.

References

- [1] C. Evangeline, V. Pragasam, K. Rambabu, S. Velu, P. Monash, G. Arthanareeswaran, F. Banat, Iron oxide modified polyethersulfone/cellulose acetate blend membrane for enhanced defluoridation application, *Desal. Water Treat.*, 156 (2019) 177–188.
- [2] T. Arumugham, N.J. Kaleekkal, S. Gopal, J. Nambikkattu, K. Rambabu, A.M. Aboulella, F. Banat, Recent developments in porous ceramic membranes for wastewater treatment and desalination: a review, *J. Environ. Manage.*, 293 (2021) 112925, doi: 10.1016/j.jenvman.2021.112925.
- [3] H.M. Tham, K.Y. Wang, D. Hua, S. Japip, T.Sh. Chung, From ultrafiltration to nanofiltration: hydrazine cross-linked polyacrylonitrile hollow fiber membranes for organic solvent nanofiltration, *J. Membr. Sci.*, 542 (2017) 289–299.
- [4] Ch. Ong, Gh. Falca, T. Huang, J. Liu, P. Manchanda, S. Chisca, S.P. Nunes, Green synthesis of thin-film composite membranes for organic solvent nanofiltration, *ACS Sustainable Chem. Eng.*, 8 (2020) 11541–11548.
- [5] J. Wu, M. Xia, Z. Li, L. Shen, R. Li, M. Zhang, Y. Jiao, Y. Xu, H. Lin, Facile preparation of polyvinylidene fluoride substrate supported thin film composite polyamide nanofiltration: effect of substrate pore size, *J. Membr. Sci.*, 638 (2021) 119699, doi: 10.1016/j.memsci.2021.119699.
- [6] L. Shan, J. Gu, H. Fan, S. Ji, G. Zhang, Microphase diffusion-controlled interfacial polymerization for an ultrahigh permeability nanofiltration membrane, *ACS Appl. Mater. Interfaces*, 9 (2017) 44820–44827.
- [7] Y. Song, Q. Hu, T. Li, Y. Sun, X. Chen, J. Fan, Fabrication and characterization of phosphorylated chitosan nanofiltration membranes with tunable surface charges and improved selectivities, *Chem. Eng. J.*, 352 (2018) 163–172.
- [8] K. Wang, Y. Qin, S. Quan, Y. Zhang, P. Wang, H. Liang, J. Ma, X.Q. Cheng, Development of highly permeable polyelectrolytes (PEs)/UiO-66 nanofiltration membranes for dye removal, *Chem. Eng. Res. Des.*, 147 (2019) 222–231.
- [9] X. Shan, S.L. Li, W. Fu, Y. Hu, G. Gong, Y. Hu, Preparation of high performance TFC RO membranes by surface grafting of small-molecule zwitterions, *J. Membr. Sci.*, 608 (2020) 118209, doi: 10.1016/j.memsci.2020.118209.
- [10] Z. Nadizadeh, H. Mahdavi, Grafting of zwitterion polymer on polyamide nanofiltration membranes via surface-initiated RAFT polymerization with improved antifouling properties as a new strategy, *Sep. Purif. Technol.*, 254 (2021) 117605, doi: 10.1016/j.seppur.2020.117605.
- [11] Y.T. Chung, L.Y. Ng, A.W. Mohammad, Sulfonated-polysulfone membrane surface modification by employing methacrylic acid through UV-grafting: optimization through response surface methodology approach, *J. Ind. Eng. Chem.*, 20 (2014) 1549–1557.
- [12] J. Usman, M.H.D. Othman, A.F. Ismail, M.A. Rahman, J. Jaafar, Y.O. Raji, K.A.M. Said, An overview of superhydrophobic ceramic membrane surface modification for oil-water separation, *J. Mater. Res. Technol.*, 12 (2021) 643–667.
- [13] M. Iqbal, D.K. Dinh, Q. Abbas, M. Imran, H. Sattar, A. Ahmad, Controlled surface wettability by plasma polymer surface modification, *Surfaces*, 2 (2019) 349–371.
- [14] D.J. Eyckens, K. Jarvis, A.J. Barlow, Y. Yin, L.C. Soulsby, Y.A. Wickramasingha, L.C. Henderson, Improving the effects of plasma polymerization on carbon fiber using a surface modification pretreatment, *Composites, Part A*, 143 (2021) 106319, doi: 10.1016/j.compositesa.2021.106319.
- [15] L.P. Zhu, B.K. Zhu, L. Xu, Y.-X. Feng, F. Liu, Y. Yi Xu, Corona-induced graft polymerization for surface modification

- of porous polyethersulfone membranes, *Appl. Surf. Sci.*, 253 (2007) 6052–6059.
- [16] D. Ariono, A.K. Wardani, Modification and applications of hydrophilic polypropylene membrane, *Mater. Sci. Eng.*, 214 (2017) 012014.
- [17] Z.-M. Li, Z.-K. Xu, J.-Q. Wang, J. Wu, J.-J. Fu, Surface modification of polypropylene microfiltration membranes by graft polymerization of N-vinyl-2-pyrrolidone, *Eur. Polym. J.*, 40 (2004) 2077–2087.
- [18] S. Laohaprapanon, A.D. Vanderlipe, B.T. Doma Jr., S.J. You, Self-cleaning and antifouling properties of plasma-grafted poly(vinylidene fluoride) membrane coated with ZnO for water treatment, *J. Taiwan Inst. Chem. Eng.*, 70 (2017) 15–22.
- [19] Y. Siew Khoo, W. Jye Lau, Y. Yeow Liang, M. Karaman, M. Gürsoy, A. Fauzi Ismail, A green approach to modify surface properties of polyamide thin film composite membrane for improved antifouling resistance, *Sep. Purif. Technol.*, 250 (2020) 116976, doi: 10.1016/j.seppur.2020.116976.
- [20] J. Pinson, D. Thiry, *Surface Modification of Polymers: Methods and Applications*, Wiley-VCH, German, 2020.
- [21] D.J. Miller, D.R. Dreyer, C.W. Bielawski, D.R. Paul, B.D. Freeman, Surface modification of water purification membranes, *Angew. Chem. Int. Ed.*, 56 (2017) 4662–4711.
- [22] K. Kato, E. Uchida, E.-T. Kang, Y. Uyama, Y. Ikada, Polymer surface with graft chains, *Prog. Polym. Sci.*, 28 (2003) 209–259.
- [23] Y. Uyama, K. Kato, Y. Ikada, *Grafting/Characterization Techniques/Kinetic Modeling*, Springer, Berlin, Heidelberg, 1998, pp. 1–39.
- [24] J. Zhou, Y. Lin, L. Wang, L. Zhou, B. Yu, X. Zou, H. Hu, Poly(carboxybetaine methacrylate) grafted on PVA hydrogel via a novel surface modification method under near-infrared light for enhancement of antifouling properties, *Colloids Surf., A*, 617 (2021) 126369, doi: 10.1016/j.colsurfa.2021.126369.
- [25] E. Stratakis, J. Bonse, J. Heitz, J. Siegel, G.D. Tsibidis, E. Skoulas, A. Papadopoulos, A. Mimidis, A.C. Joel, P. Comanns, J. Krüger, C. Florian, Y. Fuentes-Edfuf, J. Solis, W. Baumgartner, Laser engineering of biomimetic surfaces, *Mater. Sci. Eng.*, 141 (2020) 100562, doi: 10.1016/j.mser.2020.100562.
- [26] Ch.W. Billings, *Lasers: The New Technology of Light*, Facts on File, New York, 1992.
- [27] M. Bertolotti, *The History of the Laser*, 1st ed., CRC Press, Florida, 2004.
- [28] D. Krajcarz, Comparison metal water jet cutting with laser and plasma cutting, *Procedia Eng.*, 69 (2014) 838–843.
- [29] W. Gao, Y. Xue, G. Li, Ch. Chang, B. Li, Zh. Hou, K. Li, J. Wang, Investigations on the laser color marking of TC4, *Optik*, 182 (2019) 11–18.
- [30] V. Balzani, P. Ceroni, A. Juris, *Photochemistry and Photophysics*, Wiley-VCH, German, 2014.
- [31] D.S. Esen, N.C. Yigit, U. Tunca, G. Hizal, N. Arsu, Synthesis and characterization of multiarm (Benzoin-PS)_m-polyDVB star polymer as a polymeric photoinitiator for polymerization of acrylates and methacrylates, *J. Polym. Sci.*, 59 (2021) 2082–2093.
- [32] F. Dumur, Recent advances on visible light photoinitiators of polymerization based on indane-1,3-dione and related derivatives, *Eur. Polym. J.*, 143 (2021) 110178, doi: 10.1016/j.eurpolymj.2020.110178.
- [33] C. Pigot, G. Noirbent, D. Brunel, F. Dumur, Recent advances on push-pull organic dyes as visible light photoinitiators of polymerization, *Eur. Polym. J.*, 133 (2020) 109797. Available at: <https://www.sciencedirect.com/science/article/pii/S0014305720311101>
- [34] S.B. Mohamed-Smati, F.L. Faraj, I. Becheker, H. Berredjem, F.L. Bideau, M. Hamdi, F. Dumas, Y. Rachedi, Synthesis, characterization and antimicrobial activity of some new azo dyes derived from 4-hydroxy-6-methyl-2H-pyran-2-one and its dihydro derivative, *Dyes Pigm.*, 188 (2021) 109073, doi: 10.1016/j.dyepig.2020.109073.
- [35] Y. Li, B.O. Patrick, D. Dolphin, Near-Infrared absorbing azo dyes: synthesis and X-ray crystallographic and spectral characterization of monoazopyrroles, bisazopyrroles, and a boron-azopyrrole complex, *J. Org. Chem.*, 74 (2009) 5237–5243.
- [36] M.A. Salvador, P. Almeida, L.V. Reis, P.F. Santos, Near-infrared absorbing delocalized cationic azo dyes, *Dyes Pigm.*, 82 (2009) 118–123.
- [37] B.W. Gung, R.T. Taylor, Parallel combinatorial synthesis of azo dyes: a combinatorial experiment suitable for undergraduate laboratories, *J. Chem. Ed.*, 81 (2004) 1630–1632.
- [38] E.O. Moradi Rufchahi, H. Pouramir, H. Yousefi, Novel azo dyes derived from 8-methyl-4-hydroxyl-2-quinolone: synthesis, UV-vis studies and biological activity, *Chin. Chem. Lett.*, 24 (2013) 425–428.
- [39] H.R. Lohokare, S.C. Kumbharkar, Y.S. Bhole, U.K. Kharul, Surface modification of polyacrylonitrile based ultrafiltration membrane, *J. Appl. Polym. Sci.*, 101 (2006) 4378–4385.
- [40] Z. Liu, S. Ma, X. Li, H. Yang, Z. Xu, Porous carbonaceous composite derived from Mg(OH)₂ pre-filled PAN based membrane for supercapacitor and dye adsorption application, *J. Solid State Chem.*, 277 (2019) 493–501.
- [41] N.A.M. Nazri, W.J. Lau, A.F. Ismail, T. Matsuura, D. Veerasamy, N. Hilal, Performance of PAN-based membranes with graft copolymers bearing hydrophilic PVA and PAN segments in direct ultrafiltration of natural rubber effluent, *Desalination*, 358 (2015) 49–60.
- [42] Y. Qin, H. Yang, Z. Xu, F. Li, Surface modification of polyacrylonitrile membrane by chemical reaction and physical coating: comparison between static and poreflowing procedures, *ACS Omega*, 3 (2018) 4231–4241.
- [43] N.M. Hidzir, N.A.M. Radzali, I. AbdulRahman, S.A. Shamsudin, Gamma irradiation-induced grafting of 2-hydroxyethyl methacrylate (HEMA) onto ePTFE for implant applications, *Nucl. Eng. Technol.*, 52 (2020) 2320–2327.
- [44] B. Volynets, H. Nakhoda, M. Abu Ghalia, Y. Dahman, Preparation and characterization of poly(2-hydroxyethyl methacrylate) grafted bacterial cellulose using atom transfer radical polymerization, *Fibers Polym.*, 18 (2017) 859–867.
- [45] W. Tu, P. Maksym, K. Kaminski, K. Chat, K. Adrjanowicz, Free-radical polymerization of 2-hydroxyethyl methacrylate (HEMA) supported by a high electric field, *Polym. Chem.*, 13 (2022) 2850–2859.
- [46] K. Rambabu, S. Velu, Modified polyethersulfone ultrafiltration membrane for the treatment of tannery wastewater, *Int. J. Environ. Stud.*, 73 (2016) 819–826.
- [47] S. Velu, K. Rambabu, P. Monash, C. Sharma, Improved hydrophilic property of PES/PEG/MnCO₃ blended membranes for synthetic dye separation, *Int. J. Environ. Stud.*, 75 (2018) 592–604.
- [48] C.J. Davey, Z.X. Low, R.H. Wirawan, D.A. Patterson, Molecular weight cut-off determination of organic solvent nanofiltration membranes using poly(propylene glycol), *J. Membr. Sci.*, 526 (2017) 221–228.
- [49] A.D. Sabde, M.K. Trivedi, V. Ramachandhran, M.S. Hanra, B.M. Misra, Casting and characterization of cellulose acetate butyrate based UF membranes, *Desalination*, 114 (1997) 223–232.
- [50] D. Johnson, F. Galiano, S.A. Deowan, J. Hoinkis, A. Figoli, N. Hilal, Adhesion forces between humic acid functionalized colloidal probes and polymer membranes to assess fouling potential, *J. Membr. Sci.*, 484 (2015) 35–46.
- [51] M. Homayoonfal, A. Akbari, M.R. Mehrnia, Preparation of polysulfone nanofiltration membranes by UV-assisted grafting polymerization for water softening, *Desalination*, 263 (2010) 217–225.
- [52] X. Shi, G. Tal, N.P. Hankins, V. Gitis, Fouling and cleaning of ultrafiltration membranes: a review, *J. Water Process. Eng.*, 1 (2014) 121–138.
- [53] W. Gao, H. Liang, J. Ma, M. Han, Z.-l. Chen, Z.-s. Han, G.-b. Li, Membrane fouling control in ultrafiltration technology for drinking water production: A review, *Desalination*, 272 (2011) 1–8.
- [54] K.J. Jim, A.G. Fane, C.J.D. Fell, D.C. Joy, Fouling mechanisms of membranes during protein ultrafiltration, *J. Membr. Sci.*, 68 (1992) 79–91.
- [55] L. Song, Flux decline in crossflow microfiltration and ultrafiltration: mechanisms and modeling of membrane fouling, *J. Membr. Sci.*, 139 (1998) 183–200.